MATHEMATICA, 65 (88), N° 2, 2023, pp. 286–295

LID DRIVEN CAVITY FLOW WITH TWO POROUS SQUARE OBSTACLES

IOAN PAPUC

Abstract. The flow of Newtonian incompressible fluid inside a two-dimensional lid-driven cavity with two non-adherent porous square blocks was numerically studied. The non-linear governing equations, Darcy-Forchheimer-Brinkman for the porous medium and Navier-Stokes for the free fluid region, were solved using the finite element method. The streamlines and velocity profile of the fluid inside the cavity, as well as the maximum value of the stream function and the coordinates of the main vortex created, are investigated to determine the effect of the Reynolds number, the different combinations of Darcy number and the different placements of the porous squares, on the behaviour of the fluid flow.

MSC 2020. 76M10, 76S05.

Key words. Lid-driven cavity, incompressible fluid, porous medium, Navier-Stokes equations, stream function.

1. INTRODUCTION

The boundary value problems in bounded Lipschitz domains with interior interface between free fluid region and porous medium play a very important role in the study of transport phenomena that arises in many real life situations from natural environment and industrial systems. This is the reason why, in recent years, these problems have been intensively studied from a theoretical perspective, but especially using gradually more varied and advanced numerical methods.

Using a fictitious domain formulation, Angot investigated in [3] the flow of a viscous incompressible fluid in a fluid-porous-solid assembly by applying the Brinkman model over a fictitious porous domain that includes the whole domain being adapted according to the structure of each part (see also [4]).

Kohr et al. obtained in [9] the existence of a solution for the nonlinear Neumann-transmission problem for the Brinkman and Stokes equations in $\mathbb{R}^n, n = 2, 3$, by using a layer potential approach and the Leray-Schauder theory.

The authors thank the referee for his helpful comments and suggestions.

Corresponding author: Ioan Papuc.

DOI: 10.24193/mathcluj.2023.2.14

Also, implying results from potential theory and a fixed point theorem, Kohr et al. analysed in [10] a boundary value problem described by the Darcy-Forchheimer-Brinkman and Navier-Stokes nonlinear equations.

Two bounded Lipschitz domains in $\mathbb{R}^n, n = 2, 3$ were considered, one enclosed in another, with linear Robin type condition on the exterior boundary and linear transmission condition on the common interface between porous and free fluid regions. On the other hand, a well-known problem, encountered in a wide variety of forms and configurations, thus becoming a benchmark problem for testing new numerical methods, is the study of the fluid flow inside of a lid-driven cavity. A version of this problem that fits perfectly with our conditions is the study of the movement of a fluid in a lid-driven cavity that contains a porous obstacle inside.

Al-Amiri studied in [2], using the finite element method, the mixed-convection heat transfer in a lid-driven square cavity with heated bottom wall, containing a porous block inside. The effect that different values of Richardson number, as well as different locations and sizes of the porous block have on the heat and mass transfer is also investigated.

By applying the finite difference method, Bondarenko et al. evaluated in [5] the convective flow and heat transfer inside of a lid driven cavity with two adjacent porous blocks and filled by alumina/water nanofluid. Fluctuations in flow and heat transfer rate due to variations of the Richardson number, size of the porous blocks and concentration of solid nanoparticles were analyzed. The mixed convection was studied also by Bourada et al [6] in a lid driven square cavity having a porous obstacle on the middle of the bottom wall. The porous rectangle is maintained at a hot temperature while the sliding lid is kept at a cold temperature. The multiple-relaxation-time Lattice Boltzmann method was applied. Different values for the Darcy number, Richardson number and different shapes of porous obstacle were considered.

Our intention is to study numerically the flow of a Newtonian viscous incompressible fluid, with no temperature assumption, inside of a two-dimensional lid driven cavity with two non-adjacent porous square obstacles with different permeabilities. We also investigate the influence of the dimensionless Reynolds number, different combinations of Darcy numbers and various locations of the porous obstructions on the nature and intensity of the fluid flow.

2. MATHEMATICAL MODEL OF THE PROBLEM

A two dimensional lid-driven square cavity of dimension L, filled by a Newtonian viscous incompressible fluid is considered. Two porous square obstacles of dimension $l < L$, each of them having different permeability, are placed inside the cavity in certain locations specified by the Cartesian coordinates of their centers (x_{C_1}, y_{C_1}), (x_{C_2}, y_{C_2}).

In what follows we will denote the porous domain by $\Omega_p := \Omega_{p_1} \cup \Omega_{p_2}$ and the free fluid region by Ω_f. In addition, the exterior boundary of the domain will be denoted by Γ which will have two components, Γ_{wall}, representing the fixed vertical and bottom walls of the cavity and Γ_{lid}, the top wall that is moving to the right with a constant velocity v_{lid}. Also, for the common interface between the fluid zone and the porous medium we will use the notations: $\Gamma_1 := \partial\Omega_{p_1}$ and $\Gamma_2 := \partial\Omega_{p_2}$.

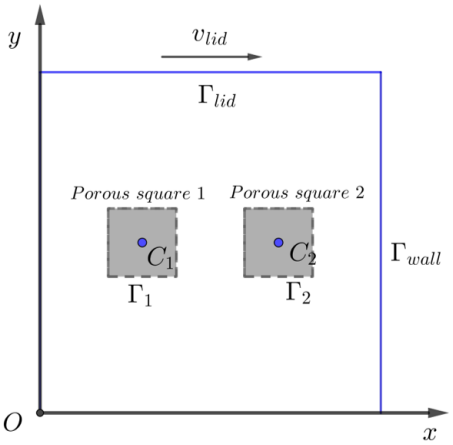

Fig. 2.1 – The lid driven cavity with 2 porous square blocks.

For the mathematical formulation of the above stated problem we will consider a couple of two well known equations in the steady-state form: the Navier-Stokes equation for the free fluid area Ω_f and the Darcy-Forchheimer-Brinkman for the porous medium Ω_p (cf. eg. [1, 8, 13, 14]). Also, the velocity and corresponding pressure are considered continuous across the interface $\Gamma_1 \cup \Gamma_2$. Hence, the system of equations and the transmission and boundary conditions that describes the flow of the fluid inside the lid driven cavity with porous obstacles is the following:

$$(1)\quad \begin{cases} \rho(\mathbf{v}\cdot\nabla)\mathbf{v} = -\nabla p + \mu\Delta\mathbf{v}, & \operatorname{div}\mathbf{v} = 0 \text{ in } \Omega_f \\ \dfrac{\rho}{\psi^2}(\mathbf{v}\cdot\nabla)\mathbf{v} = -\nabla p + \dfrac{\mu}{\psi}\Delta\mathbf{v} - \dfrac{\mu}{K_i}\mathbf{v} - \dfrac{\rho C_f}{\sqrt{K_i}}|\mathbf{v}|\mathbf{v}, & \operatorname{div}\mathbf{v} = 0 \text{ in } \Omega_{p_i} \\ \mathbf{v}_{\text{fluid}} = \mathbf{v}_{\text{porous}} & \text{on } \Gamma_i \\ p_{\text{fluid}} = p_{\text{porous}} & \text{on } \Gamma_i \\ \mathbf{v} = (v_{\text{lid}}, 0) & \text{on } \Gamma_{\text{lid}} \\ \mathbf{v} = (0,0) & \text{on } \Gamma_{\text{wall}}, \end{cases}$$

where $i = 1, 2$, ψ is the porosity and K_i denotes the permeability of the medium Ω_i, ρ and μ are the density and the dynamic viscosity of the fluid and

$$C_f = \frac{1.75}{\sqrt{150\psi^3}}$$

is the friction coefficient (cf. e.g. [12]).

Next, we use the following dimensionless variables in order to express the the dimensional equations and boundary conditions (1) in a non-dimensional form

$$X = \frac{x}{L}; \qquad Y = \frac{y}{L}; \qquad V_x = \frac{v_x}{V_0}; \qquad V_y = \frac{v_y}{V_0}; \qquad P = \frac{p}{\rho V_0^2}.$$

Note that (v_x, v_y) and (V_x, V_y) represents the components of the dimensional velocity $\mathbf{v}$ and the dimensionless one $\mathbf{V}$. Moreover, V_0 is the characteristic velocity which will be exactly the velocity v_{lid} of the moving lid.

Hence, the system of governing equations and boundary conditions (1) will have the following equivalent form:

$$(2)\quad \begin{cases} (\mathbf{V}\cdot\nabla)\mathbf{V} = -\nabla P + \dfrac{1}{\mathrm{Re}}\Delta\mathbf{V} & \text{in } \Omega_f \\ \operatorname{div}\mathbf{V} = 0 & \text{in } \Omega_f \\ \dfrac{1}{\psi}(\mathbf{V}\cdot\nabla)\mathbf{V} = -\psi\nabla P + \dfrac{1}{\mathrm{Re}}\Delta\mathbf{V} - \dfrac{\psi}{\mathrm{ReDa}_i}\mathbf{V} - \dfrac{\psi C_f}{\sqrt{\mathrm{Da}_i}}|\mathbf{V}|\mathbf{V} & \text{in } \Omega_{p_i} \\ \operatorname{div}\mathbf{V} = 0 & \text{in } \Omega_{p_i} \\ \mathbf{V}_{\text{fluid}} = \mathbf{V}_{\text{porous}} & \text{on } \Gamma_i \\ P_{\text{fluid}} = P_{\text{porous}} & \text{on } \Gamma_i \\ \mathbf{V} = (1,0) & \text{on } \Gamma_{\text{lid}} \\ \mathbf{V} = (0,0) & \text{on } \Gamma_{\text{wall}}, \end{cases}$$

Let us mention that the non-dimensional Reynolds number, denoted by Re, is defined as

$$\mathrm{Re} = \frac{V_0 L \rho}{\mu}$$

and the Darcy number, Da_i, is introduced by

$$\mathrm{Da}_i = \frac{K_i}{L^2}.$$

Moreover, we are going to consider the stream function Ψ, which is given as follows

$$(3)\qquad V_x = \frac{\partial\Psi}{\partial Y}, \qquad V_y = -\frac{\partial\Psi}{\partial X}.$$

3. NUMERICAL METHOD AND VALIDATION OF THE MODEL

The system (2), containing the couple of nonlinear equations and the transmission and boundary conditions, are solved together with the equations (3), by applying the finite element method implemented in COMSOL software.

The solution for the non-linear stationary model is obtained involving an iterative algorithm based on Newton's method, which stops when the relative tolerance falls below a given $\epsilon > 0$ which will be taken $\epsilon = 10^{-6}$ in what follows.

For the discretization of the domain, a non-uniform mesh of free quad was chosen. In order to obtain the best approximation of the solution with a relatively low computational cost, a mesh independence test was performed.

We analysed the effect of the number of boundary elements and the maximum size of the elements on the maximum value of the stream function, that was denoted by $\mathbf{\Psi}_{\max} := \max(|\Psi|)$. Hence, for the case when the non-dimensional parameters were set at the following values

$$\mathrm{Re} = 100, \quad \mathrm{Da}_1 = \mathrm{Da}_2 = 0.1, \quad \psi = 0.3, \quad l = 0.2,$$
$$(x_{C_1}, y_{C_1}) = (0.3, 0.5), \quad (x_{C_2}, y_{C_2}) = (0.7, 0.5),$$

and a number of 8 different configurations of the mesh were considered within the range of 25×25 and 150×150 elements. The effect of the grid size is observed in Table 1, where the values of $\mathbf{\Psi}_{\max}$ computed for each corresponding case seem to converge to a certain value as the number of boundary elements increases. Hence, the grid with 150 elements on the boundary looks appropriate, so it will be chosen for the further simulations.

Table 1 – Mesh dependence of the maximum stream function value.

Elements on the boundary	$\mathbf{\Psi}_{\max}$	$\mathbf{Error}_{\mathbf{\Psi}_{\max}}$
25	0.10803411	
50	0.10822701	192.9×10^6
75	0.10824833	21.32×10^6
100	0.10825726	8.93×10^6
125	0.10825251	4.75×10^6
150	0.10825247	0.04×10^6

In order to verify if our approach is valid, we need to compare the obtained results with those existing in the literature. To this end we are going to set the porosity at $\psi = 0.999$ and the non-dimensional Darcy number for both porous squares to $\mathrm{Da} = 10^5$. In this way, our problem approximates with a fairly good accuracy the classical lid-driven cavity flow problem, containing only free fluid inside, without any porous medium assumption. Consequently, the validation of the method can be done by comparing our solution with those obtained for the study of free fluid flow governed only by the Navier-Stokes equations.

For different values of the Reynolds number, we have included in Table 2 the maximum value of the stream function and the coordinates of the location where this value is reached. Table 2 shows a good agreement between the results obtained in this paper and those reported in [7] and [11].

Table 2 – Comparison of $\mathbf{\Psi}_{\max}$ and $(x_{\mathbf{\Psi}_{\max}}, y_{\mathbf{\Psi}_{\max}})$ for the classical lid driven cavity.

Re	**100**	**400**	**1000**
Present paper	0.103522	0.114012	0.119127
	(0.613,0.738)	(0.552,0.605)	(0.528,0.566)
Ghia et al. [7]	0.103423	0.113909	0.117929
	(0.617, 0.734)	(0.554,0.605)	(0.531,0.562)
Marchi et al. [11]	0.103521	0.113988	0.118936
	(0.616,0.737)	(0.553,0.605)	(0.531,0.565)

4. RESULTS AND DISCUSSION

In what follows, our aim is to study the effects that the Reynolds number, the Darcy number and the locations of the porous obstacles produce on the behaviour of the fluid inside the cavity.

Numerical investigations are performed for the following values $1 \leq \mathrm{Re} \leq 500$, $0.001 \leq \mathrm{Da}_1, \mathrm{Da}_2 \leq 10$, and $x_{C_1}, y_{C_1}, x_{C_2}, y_{C_2} \in \{0.3, 0.5, 0.7\}$, where C_1, C_2 denotes the centers of the porous squares. Meanwhile, the other non-dimensional parameters are kept to their default values $L = 1$, $l = 0.2$ and $\psi = 0.3$.

The mass transport phenomena will be analysed based on the velocity profiles of the particles of fluid and stream lines displayed in the figures, as well as on the maximum values of the stream function and the coordinates of the main vortexes, which will be included in tables.

4.1. THE EFFECT OF THE REYNOLDS NUMBER

First we evaluate the impact of the non-dimensional Reynolds number on the flow of the fluid in the lid driven cavity. Taking the same permeability in both square obstacles, $\mathrm{Da}_1 = \mathrm{Da}_2 = 0.1$, and keeping them at a fixed positions $C_1(0.3, 0.5)$, $C_2(0.7, 0.5)$, we set the following values for Re: $1, 50, 100, 200, 250, 300, 400, 450, 500$.

As we can see in Figure 4.2, for low values of Reynolds number, the flow of the fluid is laminar and it becomes turbulent as Re increases, creating a second vortex in the lower right corner and even a third one in left corner.

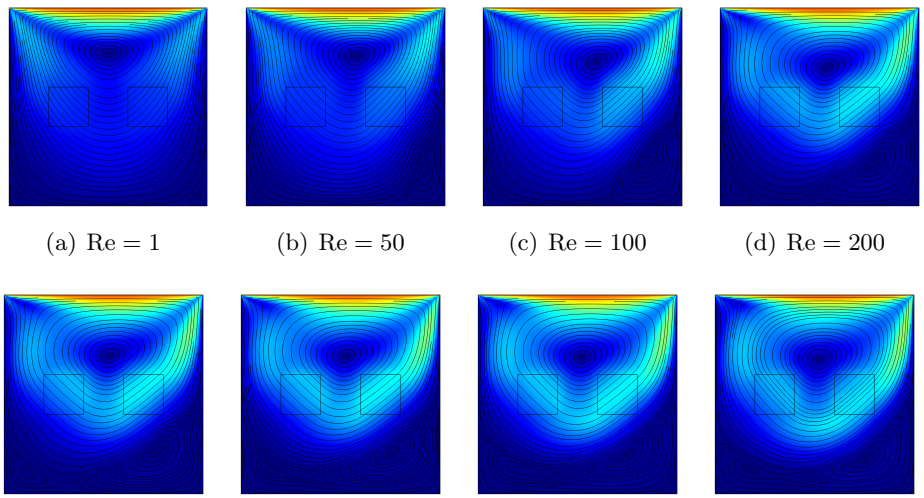

(a) Re = 1 (b) Re = 50 (c) Re = 100 (d) Re = 200

(e) Re = 250 (f) Re = 300 (g) Re = 400 (h) Re = 500

Fig. 4.2 – Velocity and streamlines for $\psi = 0.3$, $\mathrm{Da}_1 = \mathrm{Da}_2 = 0.1$, $C_1(0.3, 0.5)$, $C_2(0.7, 0.5)$ and different values of Re.

As the value of 300 is reached and exceeded, the two vertices at the bottom of the cavity join and form a new cell that is significant in size. Due to the presence of the porous medium with the configuration and permeability specified above, the value 500 is the highest for which a solution can be obtained using the stationary model. Also, Table 3 suggests that the higher value for the stream function is obtained when Re = 450.

Table 3 – Dependency of $\mathbf{\Psi}_{\max}$ on Re.

Re	$\mathbf{\Psi}_{\max}$	Main vortex center $(x_{\mathbf{\Psi}_{\max}}, y_{\mathbf{\Psi}_{\max}})$
1	0.095735	(0.501,0.771)
50	0.100608	(0.557,0.755)
100	0.108252	(0.570,0.731)
200	0.118755	(0.541,0.701)
250	0.122021	(0.530,0.694)
300	0.124257	(0.525,0.694)
400	0.126472	(0.522,0.688)
450	0.126702	(0.521,0.684)
500	0.125771	(0.526,0.678)

4.2. THE EFFECT OF DARCY NUMBERS

Now we consider the fixed values of Re = 100 and $(x_{C_1}, y_{C_1}) = (0.3, 0.5)$, $(x_{C_2}, y_{C_2}) = (0.7, 0.5)$, and we set the permeabilities of the porous squares at different values given by their corresponding Darcy numbers: $\mathrm{Da}_1 = 10$, 10^{-1}, 10^{-3} and $\mathrm{Da}_2 = 10$, 10^{-1}, 10^{-3}.

It can be seen in Figure 4.3 that for higher values of Da, the small squares do not slow down the fluid, which penetrates the porous medium without encountering significant opposition. On the other hand, for Da tending to zero, the porous obstacle begins to behave like a blockage, the low velocity of the fluid in the porous media being highlighted in Figure 4.3 (c), (e), (f), (g) by the dark blue color. Another important aspect that can be observed in Figure 4.3 is the laminar character of the fluid movement in each of the 3 cases with $\mathrm{Da}_2 = 10^{-3}$. No vortex can be seen in images (c), (e), (h), because the second obstacle blocks the flow of fluid that is engaged by the sliding of the top wall of the cavity. The same conclusion can be drawn from Table 4, where the third column contains the lowest values of $\mathbf{\Psi}_{\max}$, which means that the second square has a much higher efficiency in changing the flow intensity.

Table 4 – Dependency of $\mathbf{\Psi}_{\max}$ on Da_1 and Da_2.

$\mathrm{Da}_1 \setminus \mathrm{Da}_2$	**10**	$\mathbf{10^{-1}}$	$\mathbf{10^{-3}}$
10	0.109073 (0.564;0.725)	0.1086107 (0.564;0.725)	0.082496 (0.660;0.806)
$\mathbf{10^{-1}}$	0.108714 (0.564;0.725)	0.108252 (0.570;0.731)	0.082405 (0.660;0.806)
$\mathbf{10^{-3}}$	0.093812 (0.626;0.767)	0.093566 (0.626;0.767)	0.078498 (0.673;0.817)

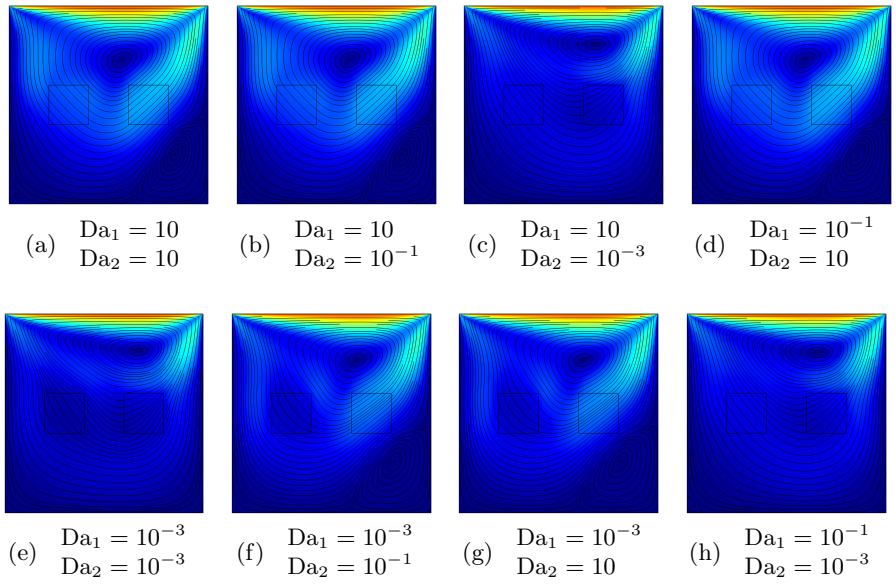

Fig. 4.3 – Velocity and streamlines for $\psi = 0.3$, $\mathrm{Re} = 100$, $C_1(0.3, 0.5)$, $C_2(0.7, 0.5)$ and different values of Da_1 and Da_2.

4.3. THE EFFECT OF THE LOCATION OF THE POROUS BLOCKS

Next, we assume that $\mathrm{Re} = 100$ and both porous squares have the same permeability $\mathrm{Da}_1 = \mathrm{Da}_2 = 0.1$ and we study the influence of the position of the obstacles inside the cavity on the trajectories of the fluid particles and on the maximum stream function value. Hence, we consider the following values for the Cartesian coordinates of the centers of the square obstacles $C_1(x_{C_1}, y_{C_1})$, $C_2(x_{C_2}, y_{C_2}) : 0.3, 0.5, 0.7$. The combinations and configurations formed with these coordinates can be found in Table 5.

Table 5 – Dependency of $\mathbf{\Psi}_{\max}$ on the position of $C_1(x_{C_1}, y_{C_1})$, $C_2(x_{C_2}, y_{C_2})$-coordinates of the square centers.

$(x_{C_1}, y_{C_1})/\ (x_{C_2}, y_{C_2})$	$\mathbf{\Psi}_{\max}$	$(x_{\mathbf{\Psi}_{\max}}, y_{\mathbf{\Psi}_{\max}})$
(0.3,0.3) / (0.7,0.3)	0.102555	(0.617,0.743)
(0.3,0.5) / (0.7,0.5)	0.108252	(0.570,0.731)
(0.3,0.7) / (0.7,0.7)	0.093035	(0.576,0.686)
(0.3,0.3) / (0.3,0.7)	0.096544	(0.636,0.762)
(0.5,0.3) / (0.5,0.7)	0.088332	(0.630,0.805)
(0.7,0.3) / (0.7,0.7)	0.095640	(0.546,0.66)
(0.3,0.3) / (0.7,0.7)	0.093992	(0.563,0.679)
(0.3,0.7) / (0.7,0.3)	0.098265	(0.635,0.754)

Figure 4.4 shows the impact that the placement of porous bodies has on fluid movement. In most cases, there is a reduction in turbulence, the most obvious being situations (a) and (f) where the flow becomes completely laminar. Also, the configuration (f), in which the obstacles are placed in the middle of the cavity, one above the other, generates the lowest value of the stream function, which can be found in Table 5, and which proves a reduction of fluid flow in the enclosure.

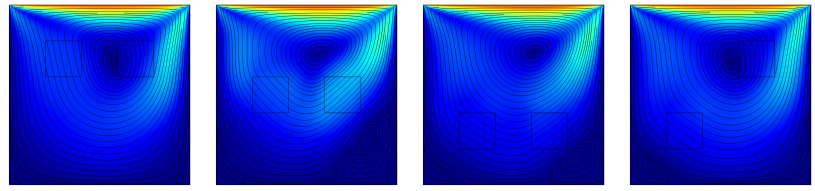

(a) $C_1(0.3, 0.7)$ $C_2(0.7, 0.7)$ (b) $C_1(0.3, 0.5)$ $C_2(0.7, 0.5)$ (c) $C_1(0.3, 0.3)$ $C_2(0.7, 0.3)$ (d) $C_1(0.3, 0.3)$ $C_2(0.7, 0.7)$

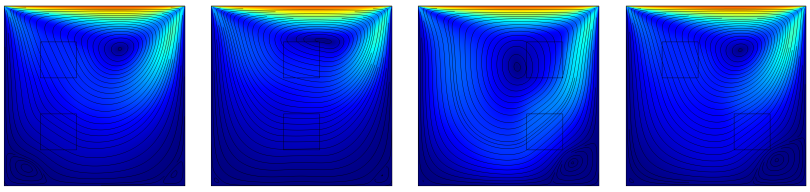

(e) $C_1(0.3, 0.3)$ $C_2(0.3, 0.7)$ (f) $C_1(0.5, 0.3)$ $C_2(0.5, 0.7)$ (g) $C_1(0.7, 0.3)$ $C_2(0.7, 0.7)$ (h) $C_1(0.3, 0.7)$ $C_2(0.7, 0.3)$

Fig. 4.4 – Velocity and streamlines for $\psi = 0.3$, Re $= 100$, $\mathrm{Da}_1 = \mathrm{Da}_1 = 0.1$ and different location of C_1 and C_2

5. CONCLUSION

The flow of a Newtonian incompressible fluid inside a square cavity with sliding lid, containing inside two non-adherent porous block with different permeabilities, were studied numerically. The effect of different values of Reynolds number, as well as different combinations of Darcy number associated to each porous block and various locations of the obstruction in the movement of the fluid is analysed.

The investigation on the changes that occur in the pattern of the stream lines, in the velocity profile and on the maximum values of the stream function shows that flow rate increases as the Reynolds number increases and decreases as the Darcy number decreases. Similar effects can also be obtained by conveniently placing obstacles inside the cavity, placing them vertically in the middle or horizontally at the top will reduce the velocity and the turbulence.

REFERENCES

[1] A. M. Al-Amiri, *Analysis of momentum and energy transfer in a lid-driven cavity filled with a porous medium*, Int. J. Heat Mass Transfer, **43** (2000), 3513–3527.

[2] A. M. Al-Amiri, *Implication of placing a porous block in a mixed-convection heat-transfer, lid-driven cavity heated from below*, Journal of Porous Media, **16** (2013), 367–380.

[3] P. Angot, *Analysis of singular perturbations on the Brinkman problem for fictitious domain models of viscous flows*, Math. Methods Appl. Sci., **22** (1999), 1395–1412.

[4] P. Angot, *A fictitious domain model for the Stokes/Brinkman problem with jump embedded boundary conditions*, C. R. Math. Acad. Sci. Paris, **348** (2010), 697–702.

[5] D. S. Bondarenko, M. A. Sheremet, H. F. Oztop and N. Abu-Hamdeh, *Mixed convection heat transfer of a nanofluid in a lid-driven enclosure with two adherent porous blocks*, Journal of Thermal Analysis and Calorimetry, **135** (2019), 1095–1105.

[6] A. Bourada, K. Bouarnouna, A. Boutra, M. Benzema and Y. K. Benkahla, *Numerical simulation of mixed convection in a lid driven cavity with porous obstacle using (MRT-LBM)*, in *2nd National Conference on Computational Fluid Dynamics & Technology (CFD & Tech)*, 2018.

[7] U. Ghia, K.N. Ghia and C.T. Shin, *High-Re Solutions for incompressible flow using the Navier-Stokes equations and a multigrid method*, J. Comput. Phys., **48** (1982), 387–411.

[8] Z. Guo and T. S. Zhao, *Lattice Boltzmann model for incompressible flows through porous media*, Phys. Rev. E, **66** (2002), 1–9.

[9] M. Kohr, M. L. de Cristoforis and W. L. Wendland, *Nonlinear Neumann-transmission problems for Stokes and Brinkman equations on Euclidean Lipschitz domains*, Potential Anal., **38** (2013), 1123–1171.

[10] M. Kohr, M. L. de Cristoforis and W. L. Wendland, *On the Robin-transmission boundary value problems for the nonlinear Darcy-Forchheimer-Brinkman and Navier-Stokes systems*, J. Math. Fluid Mech., **18** (2016), 293–329.

[11] C. H. Marchi, R. Suero and L. K. Araki, *The lid-driven square cavity flow: numerical solution with a* 1024×1024 *grid*, Journal of the Brazilian Society of Mechanical Sciences and Engineering, **31** (2009), 186–198.

[12] K. Vafai, *Convective flow and heat transfer in variable-porosity media*, J. Fluid Mech., **147** (1984), 233–259.

[13] S. Whitaker, *The Forchheimer equation: a theoretical development*, Transport in Porous Media, **25** (1996), 27–61.

[14] D. Yang, Z. Xue and Z. Mahias, *Analysis of momentum transfer in a lid-driven cavity containing a Brinkman-Forchheimer medium*, Transport in Porous Media, **92** (2012), 101–118.

Received April 9, 2022
Accepted June 22, 2022

Babeș-Bolyai University
Department of Mathematics
1 M. Kogălniceanu St.
400084, Cluj-Napoca, Romania
E-mail: ioan.papuc@math.ubbcluj.ro
https://orcid.org/0000-0003-4677-1882